Abstract

For the ATHENA Wide Field Imager (WFI), response files for the current options were created. This document describes the assumptions made and lists the different versions.

Change Record

Issue	*Date*	*Description of Change*	*Affected Pages*
1	2014 December 10	Initial Release	All
2	2015 February 04	Added section on Readout Threshold	7-11
3	2015 March 17	Updated new configuration	5,6,7,11,12
4	2015 March 26	Updated RMF	6,7,12

Distribution List

Organization	*Name*	*Organization*	*Name*	*Organization*	*Name*
SRON	J.-W. den Herder	IRAP	D. Barret	MPE	K. Nandra
MPE	A. Rau	UoL	D. Willingale	ECAP	J. Wilms

Approvals

Function	*Name*	*Date*	*Signature*
Author	T. Brand	26 March 2015	N/A
Author	T. Dauser	26 March 2015	N/A

Contents

List of Figures **3**

List of TBD Issues **3**

List of TBC Issues **3**

1 Introduction **5**

2 ARF **5**
2.1 Mirror Area 5
2.2 Quantum Efficiency 6
2.3 ARF Construction 6

3 RMF **7**
3.1 Currently used RMF 7
3.2 Influence of the readout threshold 8
3.3 Gaussian charge cloud density profile 10

4 RSP **12**

5 Conclusion **12**

List of Figures

1 The mirror area data provided by R. Willingale and D. Lumb with the blanket factor of 0.9. . . 5
2 The quantum efficiency data provided by A. Rau. 6
3 The final ARFs for all cases. On the left hand side, the quantum efficiency includes no external filter (case **1**), on the right hand side, it includes the external filter (case **2**). 7
4 The width of the RMF in the relevant energy range. 7
5 The geometrical situation of a charge cloud in a pixel. The charge cloud is centered at the origin. The pixel center is located at (c_x, c_y). 8
6 The charge cloud is mostly split between the direct neighbours. 9
7 The area between the two curves is proportional to the probability of a true energy E being reconstructed as $E_{low} \leq E < E_{high}$. 10
8 The influence of the readout threshold is visualized on this plot. The figure on the left hand side depicts the spatial distribution of the ideally reconstructed energy fraction over the upper-left quarter of a pixel. The histogram on the right hand side shows the histogram of the reconstructed energy at uniform randomly distributed sample points. The relative size of the charge cloud to the pixel is $11 \times 10^{-6}/130 \times 10^{-6}$, and the readout threshold is 0.1 of the incident photon energy. 11
9 The same as Fig. 8, but with a readout threshold of 0.5 of the incident photon energy. 11
10 The same as Fig. 8, but with a readout threshold of 0.8 of the incident photon energy. 12

List of TBD Issues

List of TBC Issues

List of Acronyms

ARF: Ancillary Response File
Athena: Advanced Telescope for High ENergy Astrophysics
PSF: Point Spread Function
RMF: Redistribution Matrix File
WFI: Wide Field Imager

Documentation

Reference Documents

RD1	*Athena*+ Response Files (Brand, T.)	ECAP-ATHENA+-20140210

Reference Articles

Schmid C., den Herder J.W., 2013, Athena+ Response Files, Technical report, ECAP, Bamberg

1 Introduction

For simulations of astronomical observations with the *Athena* WFI, calibration files such as the ARF, RMF, or their product, the RSP, are needed. In this document, we describe the current set of ARFs, RMFs and RSPs which can be used in such simulations.

2 ARF

The WFI ARF is composed of two inputs: The mirror area and the instrument quantum efficiency.

2.1 Mirror Area

The mirror area information have been provided by R. Willingale and D. Lumb on March 15th 2015, and describes four cases:

- Case **1**: Mirror module radius R_{max} = 1469 mm, 2.3 mm rib spacing, on-axis case.
  File: `1469_2.3_irb4c_area_vs_kev.dat`
- Case **2**: Mirror module radius R_{max} = 1469 mm, 2.3 mm rib spacing, FoV average (see comment below).
  File: `1469_2.3_irb4c_area_vs_kev.fov`
- Case **3**: Mirror module radius R_{max} = 1190 mm, 2.3 mm rib spacing, on-axis case.
  File: `1190_2.3_irb4c_area_vs_kev.dat`
- Case **4**: Mirror module radius R_{max} = 1190 mm, 2.3 mm rib spacing, FoV average (see comment below).
  File: `1190_2.3_irb4c_area_vs_kev.fov`

Files 2 and 4 are averaged over the quadratic 40×40 arcmin^2 FoV, correcting for an assumed 7 mm gap between the four quadrants of the WFI, and the influence of a constant 5 arcsecond PSF over the entire FoV.
A blanket factor of 0.9 for contingency and manufacturing errors in the mirror is already included in the data files for cases 2 and 4 and has been multiplied to the data files of cases 1 and 3. The mirror areas with the blanket factor are shown in Fig. 1.

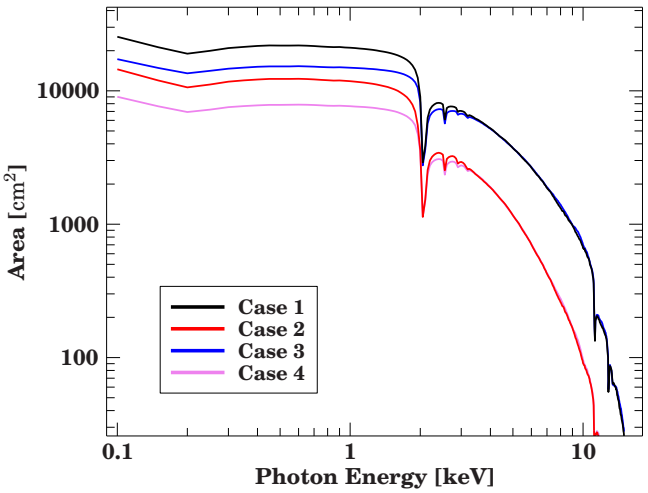

Figure 1: The mirror area data provided by R. Willingale and D. Lumb with the blanket factor of 0.9.

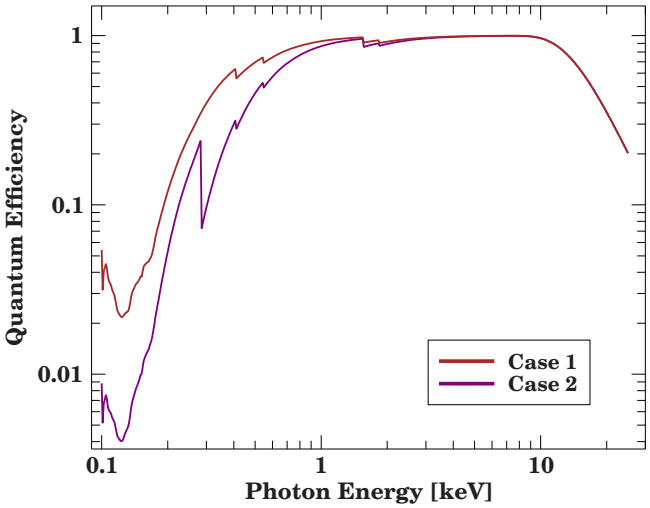

Figure 2: The quantum efficiency data provided by A. Rau.

Table 1: The filenames for the six different cases of the WFI ARF.

Mirror case	Quantum Eff. case	ARF file name
1	**1**	`athena_wfi_1469_onaxis_wo_filter_v20150326.arf`
1	**2**	`athena_wfi_1469_onaxis_w_filter_v20150326.arf`
2	**1**	`athena_wfi_1469_fovavg_wo_filter_v20150326.arf`
2	**2**	`athena_wfi_1469_fovavg_w_filter_v20150326.arf`
3	**1**	`athena_wfi_1190_onaxis_wo_filter_v20150326.arf`
3	**2**	`athena_wfi_1190_onaxis_w_filter_v20150326.arf`
4	**1**	`athena_wfi_1190_fovavg_wo_filter_v20150326.arf`
4	**2**	`athena_wfi_1190_fovavg_w_filter_v20150326.arf`

2.2 Quantum Efficiency

The quantum efficiency is provided by A. Rau, for two cases:

- Case **1**: On-chip filter only. File: `WFI-eff_wo_filter.dat`
- Case **2**: On-chip filter and external filter. File: `WFI-eff_w_filter.dat`

The quantum efficiency data is shown in Fig. 2.

2.3 ARF Construction

The ARF is the result of the multiplication of the mirror area and the quantum efficiency. Table 1 lists the eight different cases and the file names. The different ARFs are plotted in Fig. 3.

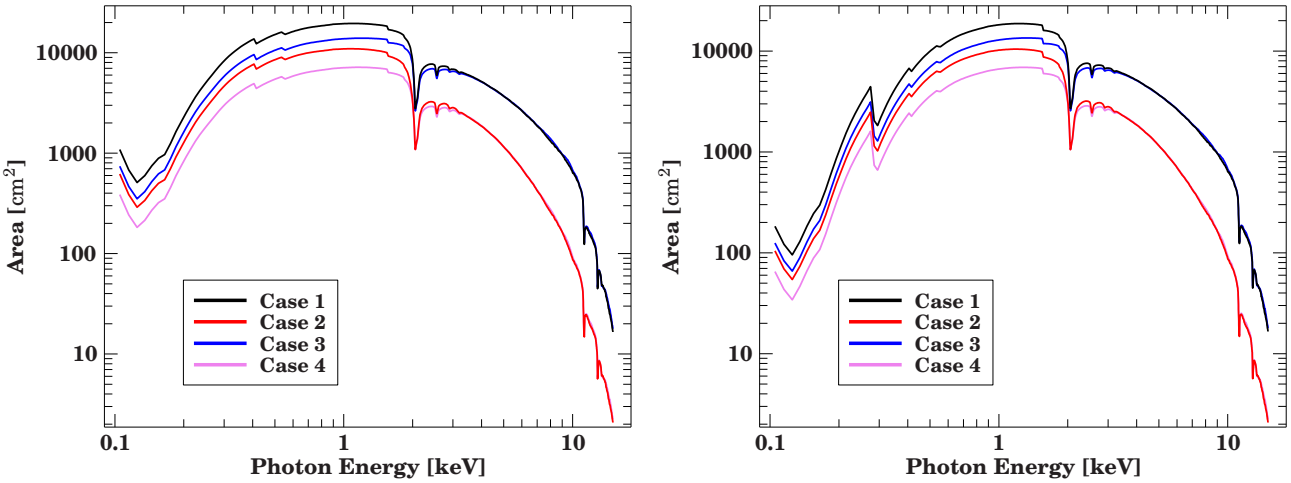

Figure 3: The final ARFs for all cases. On the left hand side, the quantum efficiency includes no external filter (case **1**), on the right hand side, it includes the external filter (case **2**).

3 RMF

3.1 Currently used RMF

The RMF has been constructed in an energy range from 0.1 keV to 15 keV with a stepsize of 0.01 keV in both Energy and EBOUNDS.
The RMF is composed of a Gaussian curve integrated in the respective EBOUNDS-bins, with a width given by the Fano-Limit with additional degradation and a noise term.
The width is described by the formula

$$\sigma = 3.65\,eV \cdot \sqrt{0.115 \times 1.15 \times E/3.65\,eV + 5^2}\ . \tag{1}$$

The resolution is shown in Fig. 4.
The RMF is now available as `athena_wfi_rmf_v20150326.rmf` .

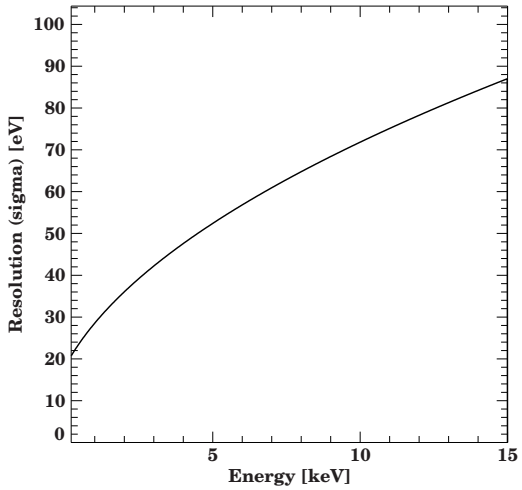

Figure 4: The width of the RMF in the relevant energy range.

3.2 Influence of the readout threshold

The RMF as implemented doe not include the low-energy-threshold. The following section describes a simple geometrical model to reproduce the effect and to visualize its influence on a measurement by calculating the resulting spectrum of a monochromatic source.
Assuming a photon generates an extended charge cloud in a pixelized detector, the generated charge may be distributed over several pixels. After the individual parts are read out, the pattern analysis finds them to belong together and sums them up to the full charge, which is an equivalent of the photon's energy.
However, due to technical constraints, the charge that can be read from an individual pixel can not be arbitrary small, but an instrument specific low-energy threshold neglects charges smaller than a given value.
The charge cloud can be represented by the total charge-energy-equivalent E_p and a normalized 2D-density function ρ,

$$E_\mathrm{p} \int_{-\infty}^{+\infty} \int_{-\infty}^{+\infty} \rho(x,y)\mathrm{dxdy} = \mathrm{E_p} \int_{0}^{+\infty} \int_{0}^{2\pi} \rho(\mathrm{r},\phi)\mathrm{r\,drd}\phi = \mathrm{E_p}\ . \tag{2}$$

Assuming the center of the charge cloud is located inside a rectangular pixel p with the corner coordinates (x_-, y_-), (x_+, y_+), the energy equivalent detected inside this pixel can be written as

$$E_0 = E_\mathrm{p} \int_{x_-}^{x_+} \int_{y_-}^{y_+} \rho(x,y)\mathrm{dxdy}\ . \tag{3}$$

Following the scheme in Fig. 5, the corner points can be expressed by the center position of the pixel $(c_\mathrm{x}, c_\mathrm{y})$ and its horizontal and vertical size, w and h:

$$\begin{aligned} x_- &= c_\mathrm{x} - w/2 \\ x_+ &= c_\mathrm{x} + w/2 \\ y_- &= c_\mathrm{y} - h/2 \\ y_+ &= c_\mathrm{y} + h/2\ . \end{aligned}$$

Assuming that the charge cloud is symmetrical along the x- and y-axis, and its characteristic width in both directions is small compared to the pixel size, it is sufficient to look at the situation in one quadrant of the pixel, as it is repeated in the other three. Here the center of the pixel will be restricted to $0 \le c_\mathrm{x} < w/2$ and $-h/2 \le c_\mathrm{y} < 0$.

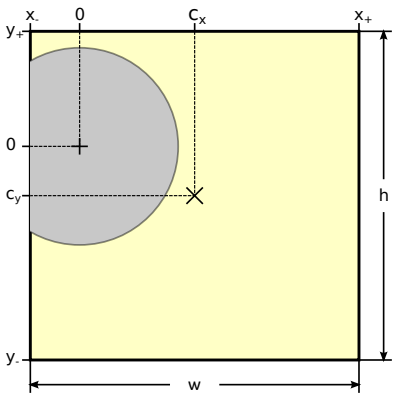

Figure 5: The geometrical situation of a charge cloud in a pixel. The charge cloud is centered at the origin. The pixel center is located at $(c_\mathrm{x}, c_\mathrm{y})$.

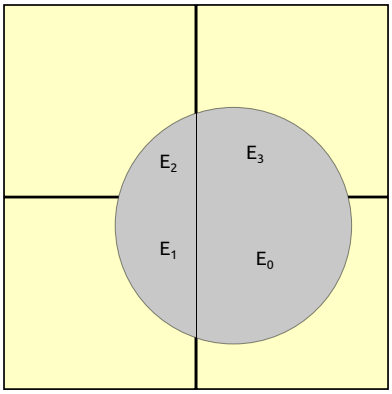

Figure 6: The charge cloud is mostly split between the direct neighbours.

The biggest portion E_0 of the charge will be found inside the pixel p, most of the remaining charge is located inside the pixels along the left and upper border, E_1, E_2, E_3, as depicted in Fig. 6. The energy equivalents are:

$$E_1 = E_0 \int_{c_x-3/2w}^{c_x-1/2w} \int_{c_y-1/2h}^{c_y+1/2h} \rho(x,y)\mathrm{dxdy} \tag{4}$$

$$E_2 = E_0 \int_{c_x-3/2w}^{c_x-1/2w} \int_{c_y+1/2h}^{c_y+3/2h} \rho(x,y)\mathrm{dxdy} \tag{5}$$

$$E_3 = E_0 \int_{c_x-1/2w}^{c_x+1/2w} \int_{c_y+1/2h}^{c_y+3/2h} \rho(x,y)\mathrm{dxdy}\ . \tag{6}$$

If the charge cloud extends even farer, the rest can be expressed by the difference to the total energy:

$$E_\mathrm{r} = E_\mathrm{p} - \sum_{i=0}^{3} E_\mathrm{i}\ . \tag{7}$$

In this situation, a low-energy readout threshold will neglect all partial charges with a energy equivalent smaller than a given E_t. With the previous assumption, E_r is allways smaller than E_t and can be neglected from now on. The measured energy after the recombination is the sum of all measured energies, or

$$E = \sum_{i=0}^{3} (E_\mathrm{i} \cdot H(E_\mathrm{i} - E_\mathrm{t}))\ , \tag{8}$$

where H is the Heavyside function

$$H(x) = \begin{cases} 0, & \text{if } x < 0 \\ 1, & \text{if } x \geq 0\,. \end{cases} \tag{9}$$

Turning around the situation, one can find a geometrical path for $(c_\mathrm{x}, c_\mathrm{y})$ over the pixel, on which E is constant and smaller than E_p.
Assuming a uniform distribution of photon impacts in the pixel p, the probability density of a photon energy E_p being wrongly reconstructed as an energy $E_\mathrm{low} \leq E < E_\mathrm{high}$ is proportional to the geometrical area between the two paths E_low and E_high, as illustrated in Fig. 7.

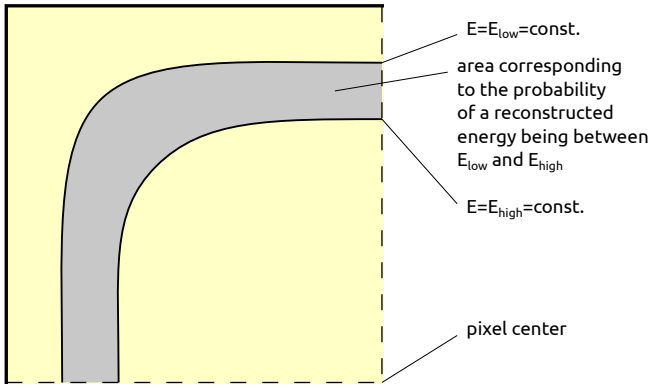

Figure 7: The area between the two curves is proportional to the probability of a true energy E being reconstructed as $E_{\mathrm{low}} \leq E < E_{\mathrm{high}}$.

3.3 Gaussian charge cloud density profile

The charge cloud density is assumed to be a 2D-Gaussian function with a width σ:

$$\rho(x,y) = \frac{1}{2\pi\sigma^2} \exp\left(-\left(\frac{x^2}{2\sigma^2} + \frac{y^2}{2\sigma^2}\right)\right) \tag{10}$$

The indefinite integral of ρ is:

$$\int\int \rho(x,y)\mathrm{dxdy} = \frac{1}{4}\mathrm{erf}(\frac{\mathrm{x}}{\sqrt{2}\sigma})\mathrm{erf}(\frac{\mathrm{y}}{\sqrt{2}\sigma}) + \mathrm{C}\ . \tag{11}$$

This can be integrated numerically and transferred into Eq. 8. To obtain the distortion of the spectrum due to the readout threshold, a large number of points on the pixel can be probed for the reconstructed energy. This makes it also possible to investigate the spatial influence of the parameters.
Fig. 8-10 show the spatial distribution of the reconstructed energy and the resulting spectra for a WFI-like pixel/charge cloud size ratio and three different threshold levels.
In Fig. 8, a low threshold of $E_{\mathrm{t}}/E_{\mathrm{p}} = 0.1$ is set. The spatial distribution shows that in the center of the pixel the full energy is recovered. Towards the edge of the pixel, the fraction of the charge in the neighbouring pixels rises but stays below the threshold, reducing the reconstructed energy. Very close to the border, the deposited charge in the neighbouring pixels becomes larger than the threshold. In this case, the reconstructed energy rises again to the incident energy. The spectrum already shows a slight degeneration, shifting a fraction of the total counts towards lower energies.
In Fig. 9, the threshold is set up to $E_{\mathrm{t}}/E_{\mathrm{p}} = 0.5$. At this value, a point at the exact border between two pixels does not allow the energy to be reconstructed at all, as the fraction of the charge in both pixels is equal to the threshold and will thus be neglected. Towards the center, the reconstructed fraction rises and is again 1 in the center of the pixel, due to the small charge cloud. The spectrum is now maximally degraded.
In Fig. 10, the threshold is set up to $E_{\mathrm{t}}/E_{\mathrm{p}} = 0.8$. At the border of the pixel a zone developed which is essentially blind to photons, as the resulting charge cloud fractions are all below the threshold. The spectrum is now better than for $E_{\mathrm{t}}/E_{\mathrm{p}} = 0.5$, but the fraction of not detected events (here shown for $E = 0$) rises.

4 RSP

The overall response files, the RSPs, are a multiplication of the ARF and the RMF. As there are eight different ARFs and one RMF, there are eight RSP files. These are listed in Table 2.

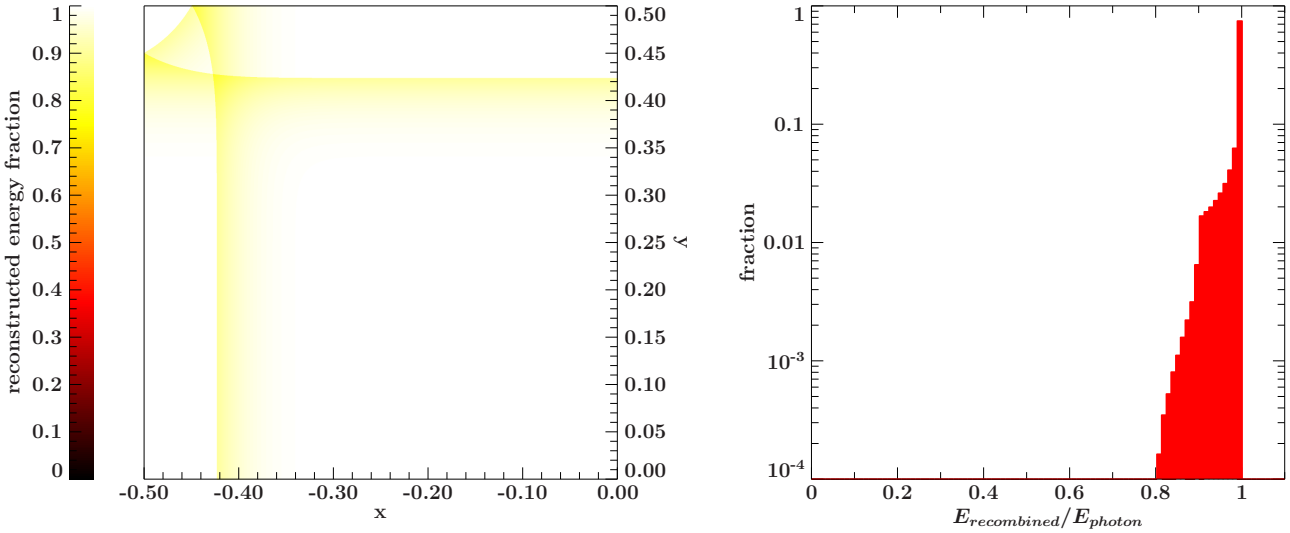

Figure 8: The influence of the readout threshold is visualized on this plot. The figure on the left hand side depicts the spatial distribution of the ideally reconstructed energy fraction over the upper-left quarter of a pixel. The histogram on the right hand side shows the histogram of the reconstructed energy at uniform randomly distributed sample points. The relative size of the charge cloud to the pixel is $11 \times 10^{-6}/130 \times 10^{-6}$, and the readout threshold is 0.1 of the incident photon energy.

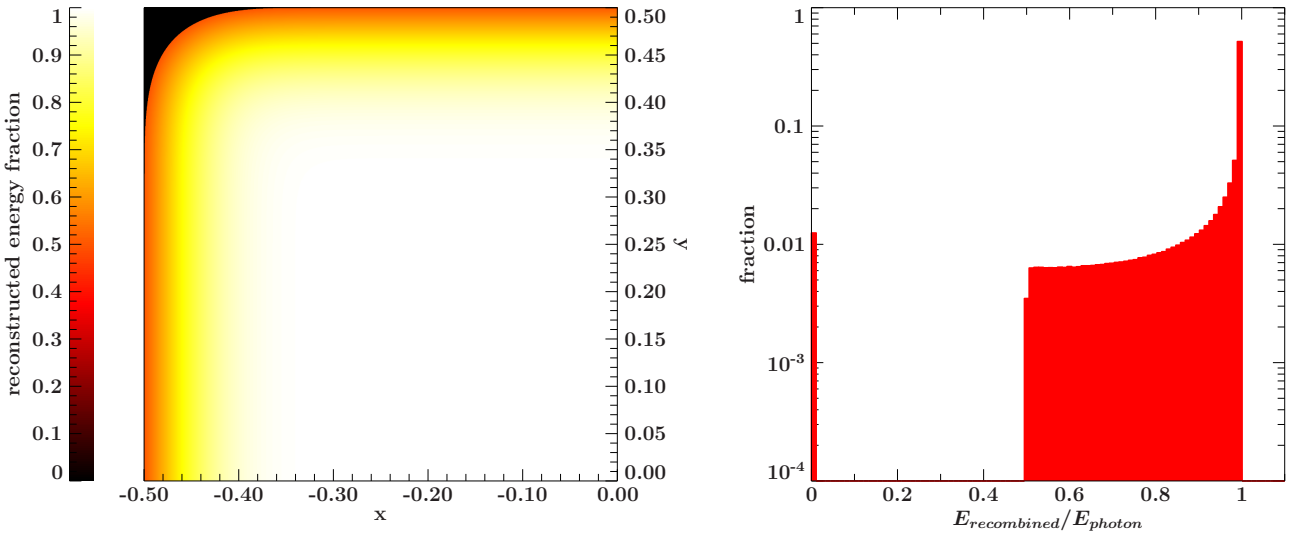

Figure 9: The same as Fig. 8, but with a readout threshold of 0.5 of the incident photon energy.

5 Conclusion

The calibration files listed in this document can be used for simulations of the *Athena* WFI.

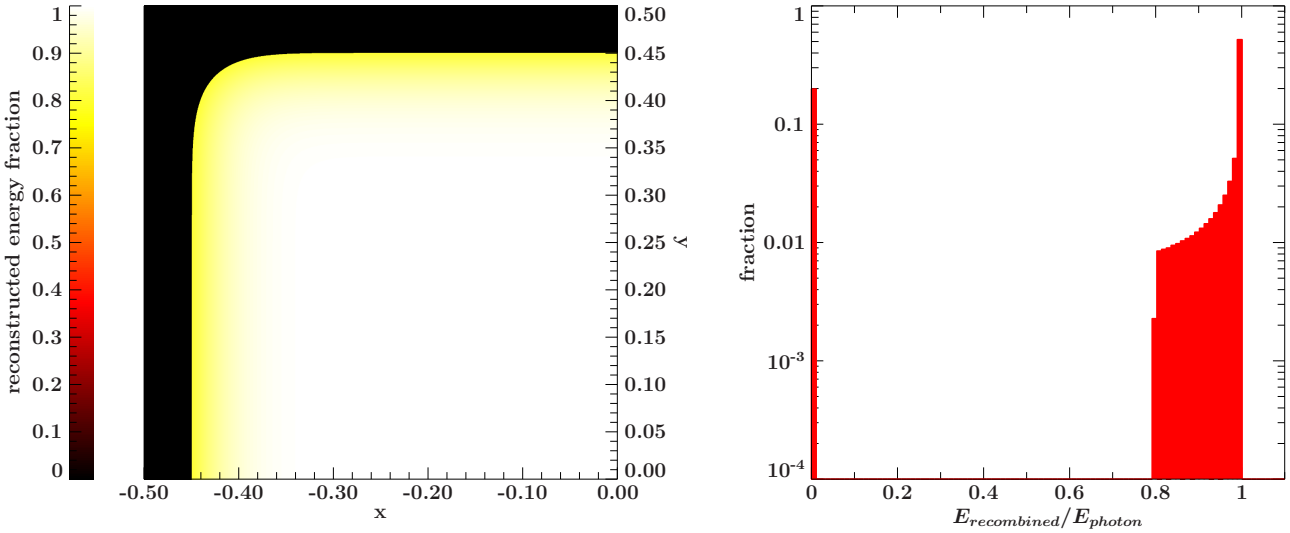

Figure 10: The same as Fig. 8, but with a readout threshold of 0.8 of the incident photon energy.

Table 2: The filenames for the eight different cases of the WFI RSP .

Mirror case	Quantum Eff. case	RSP file name
1	**1**	athena_wfi_1469_onaxis_wo_filter_v20150326.rsp
1	**2**	athena_wfi_1469_onaxis_w_filter_v20150326.rsp
2	**1**	athena_wfi_1469_fovavg_wo_filter_v20150326.rsp
2	**2**	athena_wfi_1469_fovavg_w_filter_v20150326.rsp
3	**1**	athena_wfi_1190_onaxis_wo_filter_v20150326.rsp
3	**2**	athena_wfi_1190_onaxis_w_filter_v20150326.rsp
4	**1**	athena_wfi_1190_fovavg_wo_filter_v20150326.rsp
4	**2**	athena_wfi_1190_fovavg_w_filter_v20150326.rsp